

## Estimating the seasonal predictability of global precipitation – an empirical approach

Westra, S.<sup>1</sup> and A. Sharma<sup>1</sup>

<sup>1</sup> School of Civil and Environmental Engineering, University of New South Wales, Sydney Australia.  
Email: [s.westra@unsw.edu.au](mailto:s.westra@unsw.edu.au)

**Abstract:** The asymptotic predictability of global land-surface precipitation is estimated empirically at the seasonal time scale at lead times from zero to 12 months. Predictability is defined as the maximum achievable predictive skill for a given model assuming all the relevant predictors are included and that an infinitely long training sample is available for parameter estimation, and represents an approximate upper bound to the predictive skill of statistical, and possibly dynamical, seasonal forecasting approaches. To estimate predictability, a simple linear regression model is formulated based on the assumption that land-surface precipitation variability can be divided into a component forced by low-frequency variability in external boundary conditions which potentially can be predicted one or more seasons into the future, and a ‘weather noise’ component which originates from nonlinear dynamical instabilities in the atmosphere and which is not predictable beyond about 10 days. The external boundary condition is represented by an orthogonal (principal component analysis) transformation of the global sea surface temperature anomaly (SSTA) field, as this field constitutes the dominant driver of global precipitation variability.

Predictability was estimated using the mean squared error skill score (MSESS), which has the intuitive interpretation as the reduction in variance due to the predictive model compared to a basic climatology model. The results were derived using different numbers of principal components to represent the SSTA field, as plotted in Figure 1 (black line; left axis) for up to 48 components, corresponding to 92.8% of the global SSTA variance. The increase in MSESS corresponds closely to the percentage variance of the SSTA dataset represented in the predictor pool (green line; right axis), suggesting that global precipitation variability is a direct function of SSTA variability.

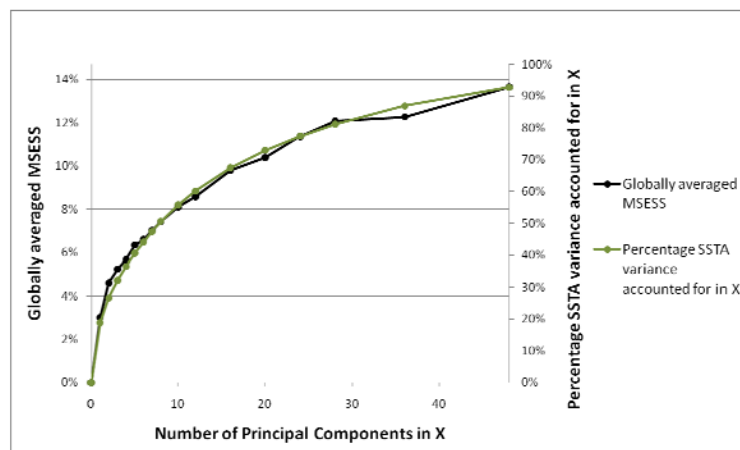


**Figure 1:** Globally averaged MSESS (left axis) and cumulative percentage variance accounted for by successive PCs (right axis).

The results in Figure 1 were extrapolated such that the asymptotic predictability using the full SSTA dataset in the predictive model was estimated to be 14.7% of the total precipitation variance. This was derived based on concurrent SSTA-precipitation relationships, and therefore constitutes the maximum skill achievable assuming perfect forecasts of the evolution of the SSTA field into the future. Imparting lags on the SSTA-precipitation relationship, the 3-, 6-, 9- and 12-month predictability of global precipitation was estimated to be 7.3%, 5.4%, 4.2%, 3.7%, respectively, demonstrating the comparative gains that can be achieved by improving SSTA forecast skill compared to developing improved SSTA-precipitation relationships. The results highlight the importance of taking the full external boundary layer variability into account rather than focusing on one or several individual climate indices. The results also demonstrate the high levels of uncertainty that are inevitably associated with seasonal forecasting, illustrating the need to ensure seasonal forecasts are described in a probabilistic manner that properly conveys predictive uncertainty.

**Keywords:** Seasonal forecasting, global precipitation, sea surface temperature, ENSO, predictability

## 1. INTRODUCTION

The field of seasonal climate forecasting has been an active area of research since Sir Gilbert Walker first discovered a relationship between large-scale atmospheric variability in the tropics and rainfall in many parts of the earth. Since this time, there have been tremendous developments in terms of conceptual understanding of the climate system, availability of large climate datasets obtained from in-situ and remotely sensed sources, together with computational resources which allow the handling of large multivariate datasets or the simulation of the dynamical equations which drive the climate system. Despite all these developments, improvements in the predictive skill for precipitation, probably the most important climate variable from a human impact perspective, has been frustratingly slow with the most sophisticated dynamical models often still not being able to outperform linear regression relationships between one or several indices that describe relevant modes variability such as the El Niño Southern Oscillation (ENSO) phenomenon, and regional precipitation (e.g. Anderson *et al*, 1999; van den Dool, 2007; Wilks, 2008).

It therefore seems appropriate to ask the question: to what extent is the global precipitation field predictable? It is well known that individual weather patterns are not predictable beyond a period of about 10 days due to the nonlinear internal dynamics of the atmosphere that effectively limits dynamical predictability beyond individual synoptic systems (e.g. Goddard *et al*, 2001; van den Dool, 2007). Although in certain cases atmospheric general circulation is predictable beyond individual weather patterns, at the seasonal time scale the majority of predictability is derived from lower-boundary forcing which evolves on a much lower time scale than individual weather systems. These boundary conditions do not allow specification of the exact timing of transitions between different weather regimes which result largely out of internal atmospheric variability, but they can influence the probability of their occurrence, thereby allowing specification of the probability of below- or above-average precipitation for lead times as long as the relevant boundary forcing can be predicted. This forms the basis for developing precipitation forecasts for lead times up to a year or even longer (Goddard *et al*, 2001).

The first step in seasonal prediction therefore is to identify a set of external boundary conditions relevant to a particular precipitation field, and attempt to describe the future evolution of these boundary conditions. A range of boundary conditions relevant to seasonal forecasting have been proposed, including sea surface temperature anomalies (SSTAs), soil moisture, vegetation, snow and sea ice cover, although these are not equally important. In particular, SSTAs have long been regarded as the principal forcing variable of atmospheric circulation (Barnston *et al*, 2005) and have been shown to influence the probabilities of below- and above-average precipitation in many parts of the world (van den Dool, 2007).

Complete knowledge of the future evolution of all relevant external boundary conditions does not, however, imply a perfect precipitation forecast. In particular, a conceptual breakdown of atmospheric circulation into a predictable component driven largely by low-frequency variations in external boundary conditions, and a ‘weather noise’ component which is unpredictable at the seasonal time scale, implies that there exists some upper limit to the seasonal predictability which cannot be improved upon even with perfect mathematical representation of the global climate system and with perfect forecasts of the future evolution of all the relevant boundary conditions. To this end, Barnston *et al* (2005) describe an approach to quantifying the upper limit to atmospheric predictability by generating ensembles of different atmospheric general circulation models (AGCMs) forced to historical boundary conditions but with differencing initial conditions to isolate the relative influences of (potentially predictable) boundary forcing and (largely unpredictable) internal atmospheric dynamics on response variables such as global precipitation. Although in many ways this represents a conceptually attractive approach able to capture the full nonlinear dynamical relationship between all the relevant external boundary variables and precipitation, the difficulty in accurately representing the fine temporal- and spatial-scale precipitation processes often lead to significant biases, which may remain even after developing ensembles of multiple AGCMs (Barnston *et al*, 2005).

In this paper we propose a simple alternative empirical approach based on linear regression methods to directly estimate the upper limit of predictive skill for global precipitation. The upper limit of predictive skill, which we will henceforth refer to as predictability, is defined within the context of our regression modelling approach as *the maximum predictive skill that can be achieved from a model assuming all relevant predictors are included and the training sample is of infinite length*. This is a statistically tractable equivalent to that proposed by Madden (1989) who defined potential predictability beyond the limit of deterministic weather predictability to be ‘the difference between the total variance of the anomalies averaged over a month or season, minus the variance that can be attributed to weather noise’. We make the assumption that the pool of relevant predictors is contained within the global SSTA field, which can be justified by the importance of this field as the dominant lower boundary forcing for precipitation. A second assumption, that the relationship

between the SSTA field and precipitation can be represented by a linear statistical model, is more difficult to justify on theoretical grounds (e.g. see Hoerling *et al*, 1997) and will probably require the type of dynamically-based analysis suggested by Barnston *et al* (2005) to confirm. As we will show, however, the linear assumption does have some grounding, and even if it proves to be theoretically unjustified, it may well provide a practical limit to seasonal prediction due to the high number of potential predictors in climate datasets and comparatively short observation records (see discussion in van den Dool, 2007).

## 2. DATA

### 2.1. Global sea surface temperature anomalies

A global sea surface temperature anomaly (SSTA) dataset was obtained from the reconstruction of raw SST values using an optimal smoother, as described in Kaplan *et al* (1998; available from <http://iridl.ldeo.columbia.edu/SOURCES/.KAPLAN/>). The data are available on a 5° longitude by 5° latitude grid across the global ocean field, totalling 1207 locations. In the temporal dimension, the data comprise monthly data which we converted to seasonal data by calculating overlapping three-month averages (i.e. DJF, JFM, FMA etc). We use data from 1900 to 2007, such that we have a record of 1296 overlapping seasons.

To facilitate linear regression modelling, the data was converted to a subset of orthogonal components using principal component analysis (PCA). The warming trend was removed by calculating the global mean SSTA value for each month of record, and subtracting this time series from the SSTA values at each location. This ensured that the principal components (time series) and eigenvectors ('loading vectors' or empirical orthogonal functions representing spatial patterns) were both mutually orthogonal.

### 2.2. Global precipitation

The Global Historical Climate Network version 2 (GHCN) gridded monthly precipitation dataset was selected as the global precipitation field to be used for this analysis (Peterson and Vose, 1997; available from <http://www.ncdc.noaa.gov/pub/data/ghcn/v2>). The dataset provides an extended coverage of global precipitation from 1900 to 2007 on a 5° longitude by 5° latitude grid, and is derived from 2064 homogeneity adjusted precipitation stations from the U.S., Canada and former Soviet Union, together with 20590 raw precipitation stations throughout the world. Prior to averaging over a 5° by 5° grid, the raw precipitation data were converted to anomaly data with respect to the 1961-1990 base period. The final gridded data comprised 819 individual grid points covering the majority of the global land surface area.

We converted the monthly precipitation data into seasonally averaged data using the same approach that was adopted for the SSTA data. There were numerous grid points, particularly over arid regions, in which a significant portion of the record between 1900 and 2007 was not reported due to insufficient data to estimate the anomaly over that location. To ensure consistency in the analysis and ensure that only high-quality data was included, all grid points which had more than 15% of the record missing for a particular season were excluded. Furthermore, to avoid statistical difficulties associated with cases where a large number of zero values were reported at a particular location and season, grid points which contained zeros for more than 5% of the record were removed. Although this process does not ensure normality in the resulting precipitation record, the prevalence of highly skewed distributions is nonetheless reduced. The result of this filtering is that, for each season, approximately 435 spatial gridded locations were included in the response dataset.

## 3. METHODOLOGY

The objective of this analysis is to estimate the upper limit of predictability of global precipitation at the seasonal time scale. To achieve this we conceptually divide the seasonal precipitation variability into two components: the first associated with variability attributable to external boundary conditions, and the second attributable to internal atmospheric variability. This second quantity is generally considered to be unpredictable beyond a period of approximately 10 days, such that at the seasonal time scale it can be described as random 'weather noise'. To this end we propose that, at any location or grid point, the rainfall time series can be partitioned into these two components, with the relationship represented by:

$$\mathbf{y} = \beta_0 + f(\mathbf{X}) + \boldsymbol{\varepsilon} \quad (1)$$

where  $\mathbf{y}$  represents the time series of precipitation at a location or grid point,  $\beta_0$  represents the sample average at that location and can be viewed as an estimator for the location climatology, and  $\boldsymbol{\varepsilon}$  represents the random 'weather noise' component. Beyond climatology, the predictable component of  $\mathbf{y}$  is contained in the term

$f(\mathbf{X})$ , where  $\mathbf{X}$  represents an  $n \times p$  matrix containing all the relevant information concerning the variability in the external boundary conditions, and  $f()$  represents some function relating  $\mathbf{X}$  to  $\mathbf{y}$ .

In addition to the assumption that precipitation at any location can be separated into a potentially predictable component related to fluctuations in external boundary conditions and a non-predictable component related to internal atmospheric variability, we make two further assumptions. These assumptions are (a) that the function  $f()$  is linear, and (b) that the matrix representing the external boundary conditions can be represented as an orthogonal representation of the SSTA dataset. Thus, Equation 1 can be simplified to yield:

$$\mathbf{y} = \beta_0 + \sum_{i=1}^p \beta_i \mathbf{x}_i + \epsilon \tag{2}$$

where  $\beta_i$  represents a  $p$ -dimensional vector of regression coefficients, and  $\mathbf{X} = [\mathbf{x}_1, \dots, \mathbf{x}_p]$  represents the PCA-transformed representation of the SSTA dataset. The PCA transform ensures that  $\mathbf{X}$  is orthogonal, and that successive components maximally represent the variance of the original data. The variance maximization property enables more than a quarter of the variance of the full 1207-dimensional global SSTA dataset to be accounted for by just the first two principal components, approximately half of the variance accounted for by the first eight components, and 90% accounted for by the first 42 components.

To estimate the maximum predictability of the precipitation data, we use the mean squared error skill score (MSESS) defined as:

$$MSESS = 1 - \frac{MSE_{pred}}{MSE_{clim}} \tag{3a}$$

where

$$MSE_{pred} = \frac{1}{(n-1-p)} \sum_{i=1}^n (y_i - \hat{y}_i)^2 \tag{3b}$$

$$MSE_{clim} = \frac{1}{(n-1)} \sum_{i=1}^n (y_i - \bar{y})^2 \tag{3c}$$

and  $n$  represents sample length indexed by  $i$ ,  $\hat{y}_i$  represents the least squares estimator for  $\mathbf{y}$  in Equation 2, and  $\bar{y}$  represents the sample mean of  $\mathbf{y}$ . The MSESS has an intuitive interpretation as the reduction in variance due to the predictive model compared to a climatology model, with a score of 1 representing a perfect model (i.e. the error term  $\epsilon$  in Equation 2 is reduced to zero), and a score of 0 representing no improvement over climatology. Dividing the model and climatology residual squared error terms in Equations 3b and 3c by  $(n-1-p)$  and  $(n-1)$  ensures that the estimators are asymptotically unbiased, which means that adding a random predictor to the model will not result in a change to the expected value of  $MSE_{pred}$ . In the remainder of this paper we express the MSESS as a percentage, by multiplying the MSESS in Equation 3a by 100.

We have now presented all the theory we intend to use for estimating the predictability for global precipitation. The model in Equation 2 is fitted to estimate  $\mathbf{y}$  from  $\mathbf{X}$ , where  $\mathbf{X}$  is of dimension  $p$  and constitutes a dimension-reduced version of the full orthogonal representation of the global SSTA dataset. This allows the MSESS to be estimated separately for each  $\mathbf{y}$  using Equation 3.

At first glance, the empirical approach described here appears overly simplistic, in particular when compared against the dynamical approach proposed by Barnston (2005). Much of the simplicity in the empirical approach stems from necessity. In particular, even though the SSTA dataset may only represent one of the boundary conditions which are likely to drive long-term precipitation variability, with other drivers including soil moisture, vegetation, snow cover and sea-ice extent, to our knowledge it is the only such dataset for which a long-term global records are available. Furthermore, we intend to apply the model in Equation 2 such that nearly 100% of the global SSTA variance is accounted for in the model, which means increasing  $p$  to approximately  $0.5 \times n$ . Adopting a nonlinear model will significantly increase the effective dimension of the predictor pool, which would prevent the development of a statistical model that explains a sufficiently large portion of the variance of the SSTA dataset to be used to estimate asymptotic predictability. As we will show, however, our empirical approach provides some interesting results which would not be possible if the assumptions are not at least approximately valid.

#### 4. RESULTS

In the previous section we discussed how estimating the MSESS using a bias-corrected MSE allows for the estimation of the maximum predictive skill that would be achievable assuming the availability of long datasets and a complete representation of the predictor pool (a detailed synthetic example is available on request). Consideration of the average value of the skill scores for a large number of response variables (i.e.

precipitation grid points) reduces the variance of this (almost) unbiased estimator, so that the best estimator of asymptotic MSESS can be achieved by considering the complete global precipitation record.

#### 4.1. Estimating Asymptotic MSESS

The asymptotic MSESS can be estimated by fitting the model described in Equation 2 separately for each precipitation grid point,  $y$ , using a common  $p$ -dimensional predictor pool contained in  $\mathbf{X}$ . The globally averaged MSESS is derived by computing the weighted average MSESS calculated at each grid point for each season, with the weighting accounting for decreasing grid size with increasing latitude. In the interests of brevity we only present the MSESS averaged over all seasons. We construct the  $p$ -dimensional predictor matrix  $\mathbf{X}$  by adding principal components sequentially in order of variance explained. Thus, for  $p = 1$ ,  $\mathbf{X} = \mathbf{x}_1$ , for  $p = 2$ ,  $\mathbf{X} = [\mathbf{x}_1 \ \mathbf{x}_2]$  and so on.

The globally averaged MSESS is calculated for  $p$  ranging from 1 to 48, where the maximum dimension of 48 was selected to be approximately half the data length. These results are plotted as a black line in Figure 1 (left axis), and show a monotonically increasing skill score with dimension. This does not represent artificial skill, as artificial skill is accounted for by using unbiased versions of the MSE to calculate the MSESS.

The first PC, which corresponds to the ENSO phenomenon, results in a globally averaged MSESS of 3%, and represents the dominant mode of seasonal predictability in the global climate. Nevertheless, there are significant increases in MSESS for higher-order PCs, up to 13.6% for all 48 PCs, suggesting that ENSO is only one of many contributors of global precipitation variability. These results are only minimally sensitive to the length of record, with slight improvements in MSESS obtained when excluding the earlier portions of the record, presumably due to decreased measurement errors in both the predictor and response fields for the second half of the twentieth century (results available on request from the authors).

The shape of the black curve in Figure 1 implies there might be a direct link between the increase in globally-averaged asymptotic MSESS and the variance of the global SSTA dataset contained in  $\mathbf{X}$ . To test this hypothesis, we also plot the variance accounted for by successive PCs as a green line in Figure 1 (right axis). We adjusted the axes such that the variance explained by the first 48 PCs lines up with the asymptotic MSESS at this dimension.

The close alignment between the two curves in Figure 1 is striking, and suggests that the improvement in the MSESS, which is interpreted as the percentage reduction in variance resulting from the fitted model relative to a baseline climatology model, is directly proportional to the fraction variance accounted for by each individual PC relative to the global SSTA field. Considering that the asymptotic global MSESS is 13.6% when using 48 PCs, which together account for 92.8% of SSTA variance, a small extrapolation brings the asymptotic MSESS accounted for by the full global SSTA dataset to 14.7%. This forms the basis for our estimate of the global predictability of seasonal precipitation.

#### 4.2. Implications of model lag

The results in Figure 1 are derived using concurrent SSTA-precipitation relationships, and we are now interested what might occur if we introduce a lagged relationship. We start by hypothesizing that precipitation variability is a function of the (approximately) instantaneous state of the SSTA field, and that any predictability at the seasonal and longer time scale is derived from the low-frequency variability in SSTA. This is physically justified by:

- (a) the importance of the global SSTA dataset in providing atmospheric boundary forcing is derived largely from the fact that the oceans contribute to approximately 85% of water vapour in the atmosphere (Bigg *et al*, 2003);
- (b) that the recycling rates (defined as the proportion of water that precipitates out because of local evaporation compared horizontal transport) is less than 10% and 20% at spatial scales of 500km and 1000km, respectively (Trenberth, 1998), implying that the majority of land-surface precipitation would be ultimately derived from evaporation from the ocean surface; and
- (c) that the residence time of water in the atmosphere is relatively short, with an  $e$ -folding residence time of atmospheric moisture calculated to be just over 8 days (Trenberth, 1998), forming the basis that the relationship between SSTA and precipitation at the seasonal time scale is approximately instantaneous.

To test this hypothesis, we first examine the persistence structure of the SSTA field. To this end we evaluate the level of persistence in each of the individual principal component time series by calculating the lag- $k$  autocorrelation coefficients with  $k$  ranging from 3 to 12 months. The results are provided in Figure 2 for up to

48 principal components, and show that as expected, the level of autocorrelation decreases with increased lag. The interesting result is that the level of autocorrelation generally also decreases with the order of the principal component. For example the first principal component, which is representative of the ENSO phenomenon, shows the maximum autocorrelation at the 3 month lag, with the level of autocorrelation gradually decreasing with the order of the PC. A spike in the autocorrelation coefficient is observed for the second principal component, and a closer examination of this PC shows that this is due to a strong trend in this component. For the remaining PCs the level of autocorrelation appears to largely decrease with the order of the PC, with autocorrelation for 6-months or longer eventually falling below the 95 percent statistically significant level of 0.2. The implications of this result for seasonal forecasting are significant, since it shows that not only does PCA provide the most efficient (in a least squares sense) representation of variability in the multivariate dataset, but it also represents the persistence structure of global SSTAs efficiently by the lower-order components.

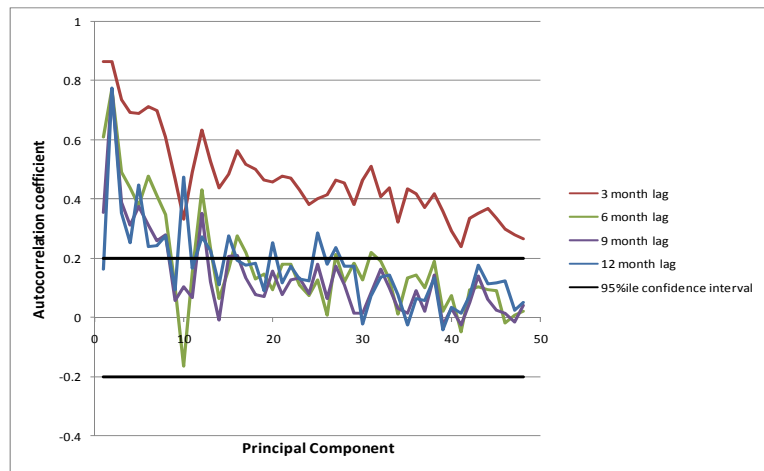


**Figure 2:** Autocorrelation coefficient against principal component for lags ranging from 3- to 12-months.

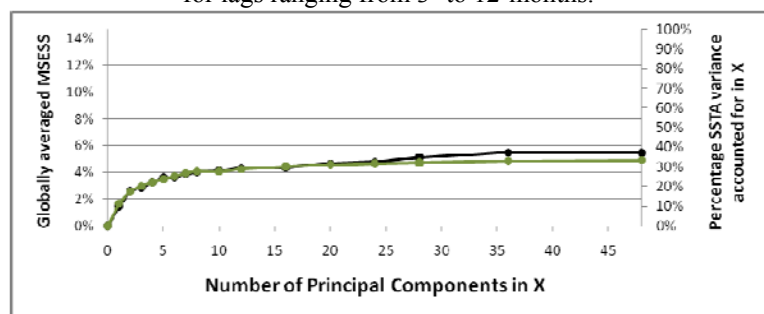


**Figure 3:** Globally averaged MSESS obtained using a 6-month lagged relationship between SSTA and precipitation (black line), and the PCA variance explained curve of the original SSTA field multiplied by the square of the autocorrelation coefficient at the same lag (green line).

If the predictable component of precipitation variability is a function of the instantaneous state of the SSTA field, then the MSESS when introducing a lag of  $k$  months should follow a curve similar to the green curve in Figure 1 multiplied by the square of the lag  $k$  autocorrelation coefficient of Figure 2. For a lag of 6 months, the theoretical relationship is given by the green line in Figure 3. As can be seen, the MSESS calculated by introducing a 6-month lag between the SSTA field and the global precipitation field, represented by the black line, follows this relationship closely. Similar results can be found for lags of 3, 9 and 12 months and are available upon request.

Due to the lower levels of autocorrelation with higher-order PCs, the maximum increases in predictability are attributable to the lowest order components, with a ‘plateauing’ of the MSESS with higher-order PCs now evident when introducing lags. This suggests that although all of the SSTA variability is relevant in representing the lower-boundary forcing of the global precipitation field, the smaller-scale fluctuations accounted for by the higher-order PCs are likely to be much less predictable, and are therefore less useful for forecasts at least one season ahead. Finally, using the same approach as before, we estimate the asymptotic MSESS by extrapolating the MSESS estimates at 48 PCs to the point where all the variability in the SSTA dataset is accounted for, and find that the asymptotic MSESS at 3, 6, 9 and 12 month lags was 7.3%, 5.4%, 4.2%, 3.7%, respectively. This indicates that significant gains in seasonal forecasting skill estimates can be derived by developing better estimates of the future evolution of the SSTA field, to an upper bound of 14.7%.

## 5. DISCUSSION AND CONCLUSIONS

In this paper we suggested a simple approach to estimating the upper bound to predictability of the global precipitation field using the global SSTA field as the principal external forcing of the global atmosphere at the seasonal timescale. We defined predictability as the maximum predictive skill, calculated through an appropriately specified statistic, which can be achieved if all the relevant predictors are included in the model

and if an infinitely long dataset were available to estimate the model parameters. We proposed that the MSESS is an intuitive statistic to measure predictability, as it represents the percentage reduction in variance achieved by a given model compared to a climatology model estimated using the sample mean.

The results of the analysis show that the upper bound to global predictability was approximately 14.7% using concurrent SSTA-precipitation relationships, with lower skill scores using lagged relationships. If the underlying assumptions of our approach can be believed, then this suggests that the majority of variability in the global precipitation field can be viewed as ‘weather noise’ (Barnston et al, 2005) and is therefore unpredictable beyond the deterministic weather ‘predictability barrier’ of approximately 10 days.

To what extent are the assumptions likely to be valid? As discussed, the primary alternative approach to determine the extent to which knowledge of SSTA forcing can result in precipitation predictability is described by Barnston *et al* (2005), and would not only provide an independent estimator of asymptotic predictability, but also shed further light on the relationship between SSTA and precipitation variability. In the absence of this information, the principal evidence that the assumptions underlying Equation 2 are approximately valid is derived empirically from our results. In particular, if the SSTA-precipitation relationship was highly nonlinear, then the relationship between variance accounted for by the PCs of the SSTA field and the MSESS would be expected to be much more complicated than that found in Figures 1 and 3. For example, the PCs which represent variability in the tropics (e.g. PC1) might account for a disproportionate amount of the variance in global precipitation compared to PCs which more evenly account for variance across all latitudes (e.g. PC2). We emphasize that we do not suggest that the SSTA-precipitation relationship is universally linear; rather, we conclude that the relationship appears to be well approximated by a locally linear (i.e. linear within the bounds of variability implied by the historical record) relationship when averaged over the global scale.

Finally, we emphasize that even if the underlying assumptions of Equation 2 are not correct (e.g. see Hoerling *et al*, 1997) and the asymptotic predictability presented in this paper underestimates true predictability, the additional predictability may not be accessible in a practical sense with the development of high-dimensional non-linear statistical models on short historical datasets being problematic. This issue may not be as valid for dynamical approaches as it is for statistical forecasting, however the difficulty in generating dynamical seasonal forecasts which outperform statistical forecasts suggests that our asymptotic estimate is likely to represent a practical upper bound for the foreseeable future (e.g. van den Dool, 2007).

## REFERENCES

- Anderson, J., van den Dool, H., Barnston, A., Chen, W., Stern, W. & Ploshay, J., 1999, Present-day capabilities of numerical and statistical models for atmospheric extra-tropical seasonal simulation and prediction”, *Bulletin of the American Meteorological Society*, 80, 1349-1361.
- Barnston, A.G., Kumar, A., Goddard, L. & Hoerling, M.P., 2005, Improving seasonal prediction practices through attribution of climate variability, *Bulletin of the American Meteorological Society*, 86 (1), 59-72.
- Bigg, G.R., Jickells, T.D., Liss, P.S. & Osborne, T.J., 2003, The role of oceans in climate. *International Journal of Climatology*, 23, 1127-1159.
- Goddard, L., Mason, S.J., Zebiak, S.E., Ropelewski, C.F., Basher, R. & Cane, M.A., 2001, Current approaches to seasonal-to-interannual climate predictions, *Int. J of Climate.*, 21: 1111-1152.
- Hoerling, M.P., Kumar, A. & Zhong, M., 1997, El Niño, La Niña and the nonlinearity of their teleconnections, *Journal of Climate*, 10: 1769-1786.
- Kaplan, A., Cane, M.A., Kushnir, Y., Clement, A.C., Blumenthal, M.B. & Rajagopalan, B., 1998, Analyses of global sea surface temperature 1856-1991. *Journal of Geophysical Research – Oceans* 102(C13): 27835-27860.
- Madden, R.A., 1989, On predicting probability distributions of time-averaged meteorological data, *Journal of Climate*, 2, 922-928.
- Peterson TC, Vose RS. 1997. An overview of the Global Historical Climatology Network temperature data base. *Bulletin of the American Meteorological Society* 78: 2837–2849.
- Trenberth, K.E., 1998, Atmospheric moisture residence times and cycling: implications for rainfall rates and climate change. *Climatic Change*, 39, 667-94.
- van den Dool, H., 2007, *Empirical Methods in Short-term Climate Prediction*. Oxford University Press, Oxford, 215 pp.
- Wilks, D.S., 2008, Improved statistical seasonal forecasts using extended training data, *International Journal of Climatology*, 28: 1589-1598.